Self-Organization of an Amphiphilic Rod−Coil−Rod Block Copolymer into Liquid Crystalline, Substrate-Supported Monolayers and Bilayers

Jee-Hyuk Kim, M. Shahinur Rahman, Jae-Suk Lee, and Ji-Woong Park*

Department of Materials Science and Engineering, Gwangju Institute of Science and Technology, Buk-gu, 1 Oryong-dong, Gwangju 500-712, Korea

Received December 4, 2007; Revised Manuscript Received February 5, 2008

ABSTRACT: We report that the amphiphilic rod−coil−rod triblock copolymer with a coil attractive to the substrate surface self-organize into liquid crystalline monolayers or bilayers of a few nanometers thickness on the substrate surface. The copolymer investigated is a triblock copolymer, poly(*n*-hexyl isocyanate-*b*-2-vinylpyridine-*b*-*n*-hexyl isocyanate) (PHIC-*b*-P2VP-*b*-PHIC). Key processes of self-organization in the thin films, such as adsorption, desorption, diffusion, nematic and smectic ordering, and microphase separation, are tuned by exposing dip- or immersion-coated nanoscale films to the vapor of solvents which are rod (PHIC)-selective, coil (P2VP)-selective, or good to both blocks. Reorganization of the rod−coils in the nanofilms yielded various morphologies in the monolayer or bilayer, including unique long-range-ordered, smectic-on-nematic biphasic sheets. The results offer understanding on the complex morphological evolution in amphiphilic rod−coil block copolymers on the substrate surface.

Introduction

Rod−coil block copolymers are a class of block copolymers obtained by covalently connecting coil-like polymers to rodlike macromolecules. In these copolymers the tendency of liquid crystalline or crystalline ordering of the rodlike chains is combined with the microphase separation between dissimilar blocks, exhibiting unique morphologies that are not found in coil−coil block copolymers.[1–6] Although their synthesis and morphological structures have been continuously studied by several groups,[5,7–9] the rod−coil block copolymers are yet to be explored further for synthesis of those with new functional architectures[10,11] and for understanding of their self-assembly processes under various chemical or physical constraints.[12–16]

A distinct structural characteristic of the self-assembled rod−coil block copolymer system is smectic-like packing of the rod blocks.[17–19] The rod blocks arrange in a smectic A- or smectic C-like fashion with their chain axes aligned normal or tilted with respect to the interface between rod and coil microdomains. The packing frustration at the rod−coil interface, which occurs owing to different interfacial areas per chain at the rod−coil junction, results in various unusual smectic microdomain morphologies in the bulk[1] or micellar morphologies in solution.[20,21] A more complicated aspect of the rod−coil self-assembly comes from the fact that their self-organization usually involves multiple ordering transitions. A lyotropic liquid crystalline state can occur during solvent evaporation from solutions prior to the final microphase-separated state.[22] Because multiple organization processes are involved, the self-assembly of a single rod−coil system can yield various morphological structures depending on the processing conditions employed.[9]

The morphological complexity and the sensitivity to processing conditions of the rod−coils may be lessened in thin films[14,23] as in the case of other types of block copolymers such as coil−coil block copolymers.[24,25] The ordering of the rod blocks in contact with the substrate surface may be controlled by the alignment or confinement effect of the surface.

One of the architectures of interest for thin film formation is an amphiphilic rod−coil block copolymer of which one of the rod and coil blocks is attractive to the substrate surface. In these rod−coils, the ordered arrangement of the rodlike blocks and the microphase separation of the rod and coil blocks occur with the adsorption of the copolymer to the substrate surface. The morphology at the substrate surface will vary according to which are more dominating factors among multiple interactions such as the copolymer−substrate adsorption interaction, the liquid crystalline or crystalline ordering of the rod blocks, and the microphase separation.[26]

At least two types of amphiphilic rod−coil copolymers can be designed depending on which part is attractive to substrate surface. The rod−coils with a surface-reactive coil is more appropriate (than those with a surface-reactive rod[27]) for utilization of the anisotropic nature of the rods on the surface. The adsorption of the rod−coils via coil−surface bonding provides a monolayer of end-grafted rods which still have rotational freedom in their azimuthal and polar anchoring angle. The grafted rods are able to respond to external stimuli and to exhibit crystalline or liquid crystalline behaviors. We reported recently that the rodlike chains tethered onto the substrate surface at a moderate grafting density yield a nematic layer with a thickness of a single chain diameter.[15]

An interesting question arises from considering that many rod−coils are known to form smectic microdomain structures[1] which are different from the nematic monolayer of the rods as bound to the substrate surface. If we deposit the rod−coils in a small excess of the monolayer thickness onto the surface, the molecules will self-assemble via many organizing processes, adsorption or desorption of the coil block, nematic ordering of the surface-bound rods, smectic ordering of unadsorbed rod−coils, and diffusion of the chains in or through the film plane. It is intriguing to see how the morphology in the film evolves as the balance between the different interactions is altered.

Here we report that the amphiphilic rod−coil−rod triblock copolymer with a coil attractive to substrate surface self-organize into liquid crystalline monolayers or bilayers of a few nanometers thickness on the substrate surface. The copolymer investigated is a triblock copolymer, poly(*n*-hexyl isocyanate-*b*-2-vinylpyridine-*b*-*n*-hexyl isocyanate) (PHIC-*b*-P2VP-*b*-PHIC). The copolymer films with thickness of a few nanometers are deposited on mica plates from toluene solutions, and then the

* Corresponding author. E-mail: jiwoong@gist.ac.kr.

10.1021/ma702695a CCC: $40.75
Published on Web 04/17/2008

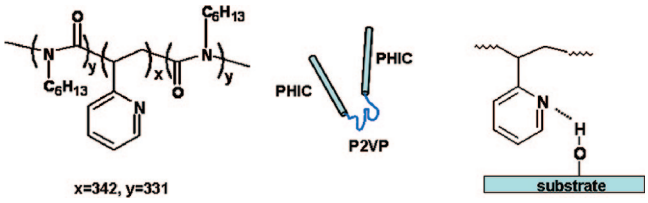

Figure 1. Chemical structure and schematic representation of $PHIC_{331}-P2VP_{342}-PHIC_{331}$ and its hydrogen-bonding adsorption onto the mica surface.

morphology in the films developed under solvent vapor-saturated atmosphere is studied by atomic force microscopy. The solvents used for vapor-annealing of the films are toluene (PHIC-selective), methanol (coil-selective), and THF (good solvent for both). The experiments yield various nanofilm morphologies including unique long-range-ordered, smectic-on-nematic biphasic sheets. The results offer new understanding on the complex morphological evolution of amphiphilic rod−coil block copolymers on the substrate surface.

Experimental Section

Materials. 2-Vinylpyridine (2VP) (Aldrich, 97%) and *n*-hexyl isocyanate (HIC) (Aldrich, 97%) were dried over CaH_2 and vacuum-distilled. Tetrahydrofuran (Fisher Scientific, GR grade) (THF) was distilled under N_2 after refluxing with sodium for 5 h and distilled again under vacuum from sodium naphthalenide solution. Calcium hydride (Junsei, 95%), naphthalene (Aldrich, 99%), sodium (Aldrich, 99%), potassium (Aldrich, 98%), sodium tetraphenylborate ($NaBPh_4$) (Aldrich, 99.5%),and diphenylmethane (Aldrich, 99%) were used without further purification.

Synthesis of Poly(*n*-hexyl isocyanate)-*b*-poly(2-vinylpyridine)-*b*-poly(*n*-hexyl isocyanate) (PHIC-*b*-P2VP-*b*-PHIC). The preparation of these triblock copolymers has been described in detail in our previous contribution. Briefly, $PHIC_{333}$-*b*-$P2VP_{342}$-*b*-$PHIC_{333}$ (M_n = 120 000, M_w/M_n = 1.13) copolymers were synthesized by sequential anionic polymerization of the comonomers. 2VP (0.86 g, 8.2 mmol) was first polymerized, at −78 °C, using the bidirectional initiator sodium naphthalenide (Na-Naph) (0.0072 g, 0.048 mmol) to provide chain growth at both ends of the macromolecule. Prior to the addition of the second monomer, a 5–10 M excess of $NaBPh_4$ (0.15 g, 0.44 mmol) was added, and the reactor cooled to −98 °C. HIC (2.032 g, 16 mmol) was then introduced, and the polymerization was carried out for 20 min. The reaction was terminated with a CH_3COOH/MeOH mixture. The reaction mixture was poured into a large amount of methanol. The precipitates were collected by filtration and dried under vacuum. Dissolution in a good solvent and precipitation in a nonsolvent were repeated to obtain pure copolymer samples. The copolymer samples were finally dissolved again in benzene and freeze-dried.

Preparation of Block Copolymer Solution. The PHIC–P2VP–PHIC block copolymer powders were dissolved in anhydrous toluene (99.8%, Aldrich) in ambient conditions. In order to vary the surface coverage, the solution concentration was varied among 1, 0.5, 0.1, 0.01, 0.005, and 0.001 wt %. The solution was filtered through 0.2 μm Teflon membrane filter before coating onto mica plates.

Deposition of Block Copolymer Films. Freshly cleaved mica substrates (Pelco, Ted pella Inc.) were obtained by carefully peeling off several layers using Scotch tape. Block copolymers were adsorbed from toluene solution onto mica plates by the dip-coating or the immersion-coating method. In dip coating, mica plates were dipped into the copolymer solution at a speed of 5 mm/s, kept in the solution for 5 s, and then pulled out from the solution at a speed of 2 mm/s, followed by repeated rinsing and washing with anhydrous toluene. In the immersion-coating method, mica plates were immersed in the copolymer solution for 3 h and then rinsed by the same procedure as in the dip-coating method.

Solvent Vapor Annealing of the Block Copolymer Film. The mica plates covered with block copolymer films were placed near a vial filled with anhydrous toluene or THF in a closed chamber for different periods of time. Then the plates were dried by exposure to the atmosphere.

Atomic Force Microscopy. Atomic force microscopy (AFM) was performed under a commercial scanning probe microscope (Digital Instruments Multimode SPM IIIa system). The AFM was equipped with a Quadrex for phase imaging and a Micro 40 active antivibration unit (Halcyonics). Tapping mode etched silicon probe (RTESP) (Veeco probe) was used for cantilever. These probes have

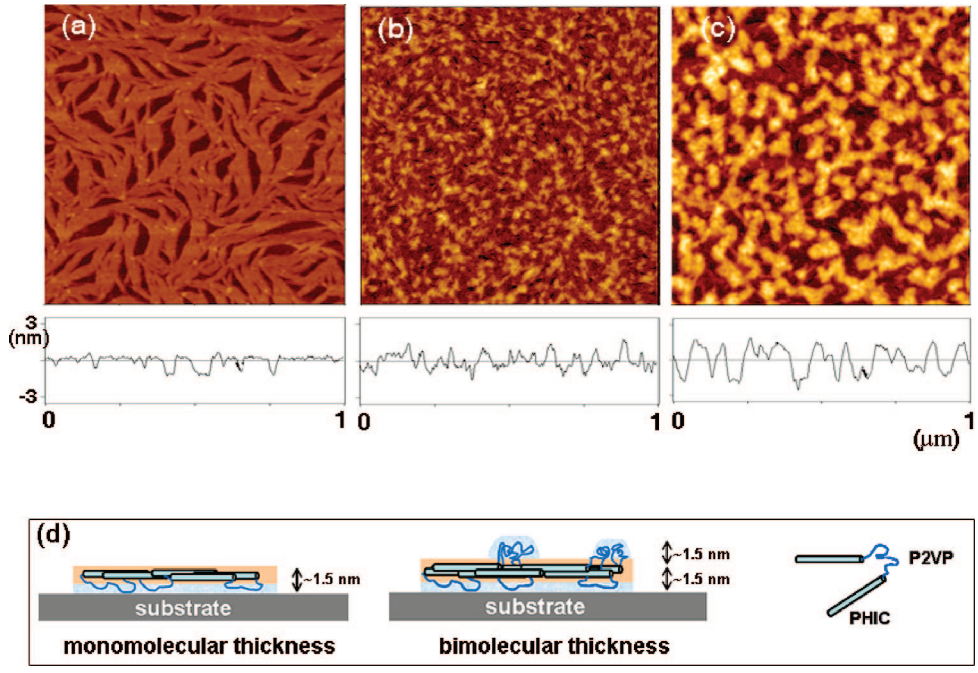

Figure 2. AFM images of as-coated films of $PHIC_{331}-P2VP_{342}-PHIC_{331}$ on mica surfaces. (a, b) The films were obtained by dip-coating in toluene solutions with the copolymer concentration of 0.1% and 1.0%, respectively. (c) The film with thicker polymer residues was obtained by immersion of the mica substrate in a 0.5% solution for 3 h. Cross-sectional profiles are given underneath each AFM image. (d) A schematic drawing for the cross-sectional structure of monomolecular and bimolecular thick films.

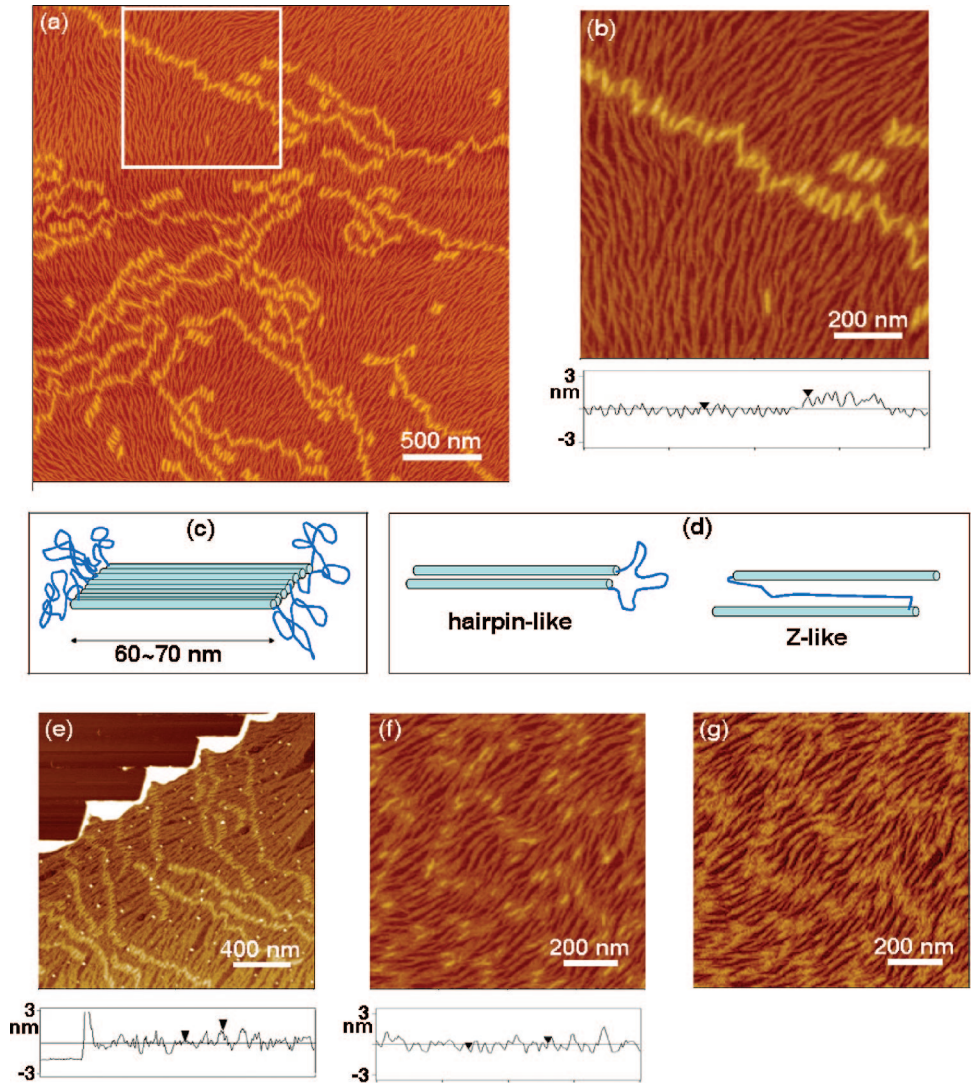

Figure 3. Formation of rod−coil bundles and their arrangement in rows on the nematic bottom monolayer surface. The films were coated by dip-coating in 0.1% toluene solution followed by annealing under THF vapor. (a) A height contrast AFM image of the film annealed for 20 h, (b) a magnified image of the square region of (a), (c) a schematic drawing of the nano-objects, (d) the copolymer molecule with hairpin-like or *z*-like conformation, respectively, (e) a height contrast AFM image obtained from the sample with upper left part scratched off by contact mode AFM scrubbing, and (f, g) respective height and phase contrast AFM images of the intermediate state obtained after THF vapor annealing for 1 h.

force constant range of 20−80 N/m and resonance frequency of 276−303 kHz. The cantilever was forced to oscillate near its resonance frequency. The laser beam was centered on the tip of the cantilever and reflected on a photodiode. To minimize the surface deformation of the sample by the tip, the so-called light tapping was applied. The layer thickness of the polymer film was determined by using contact mode atomic force microscopy. Contact mode silicon nitride tip (NP-20) (Veeco probe) with a force constant of 58 N/m was used for cantilever. An area of 1 μm × 1 μm was scanned twice with maximum force, resulting in the removal of all polymers in that particular section. Subsequently, a large-scale image (3 μm × 3 μm) was lightly scanned, including the scrubbed area surrounded by the unaffected layer using tapping mode atomic force microscopy.

X-ray Photoelectron Spectroscopy. Photoelectron spectroscopy (XPS) was performed using an ESCALAB 210 series (Thermo Electron Corp.) with Mg Kα excitation ($h\nu$ = 1253.6 eV) in an ultrahigh-vacuum (UHV, 10^{-7} Pa) system. The minimum resolution was 0.7 eV, and the analyzed area was larger than 150 μm. The binding energies referenced are from the Web site www.lasurface.com.

Results and Discussion

The block copolymer investigated is a triblock copolymer of poly(2-vinylpyridine) (P2VP) and poly(*n*-hexyl isocyanate) (PHIC), $PHIC_{331}$–$P2VP_{342}$–$PHIC_{331}$, with number-average molecular weight 120 000 and polydispersity index 1.13. The copolymer was synthesized by the anionic polymerization method reported previously.[28,29] The copolymer contains a central P2VP block that can bind to mica surface via hydrogen bonding.[30] PHIC is a helical rodlike polymer with a large persistence length of several tens of nanometers.[31] The chemical structure of the block copolymer and a schematic drawing for its adsorption onto mica surfaces are shown in Figure 1. The copolymer of 1−3 nm thickness was coated onto freshly cleaved mica plates by dip-coating in its toluene solutions followed by repeated rinsing with toluene. The grafting density of the block copolymers was adjusted by varying the concentration of dipping solutions. Relatively thick films of 3−4 nm could be obtained by immersion coating for several hours in dilute solutions of 0.001−0.5% w/v concentrations. Dip-coating in the toluene solutions with the copolymer concentration of above 1% w/v often yielded nonuniform films consisting of micellar aggregates and precipitates.

The tapping mode atomic force microscope (AFM) images of as-coated films with different amount of deposited copolymers are presented in Figure 2. Nearly full surface coverage of the substrate surface with monomolecular-thick film was attained

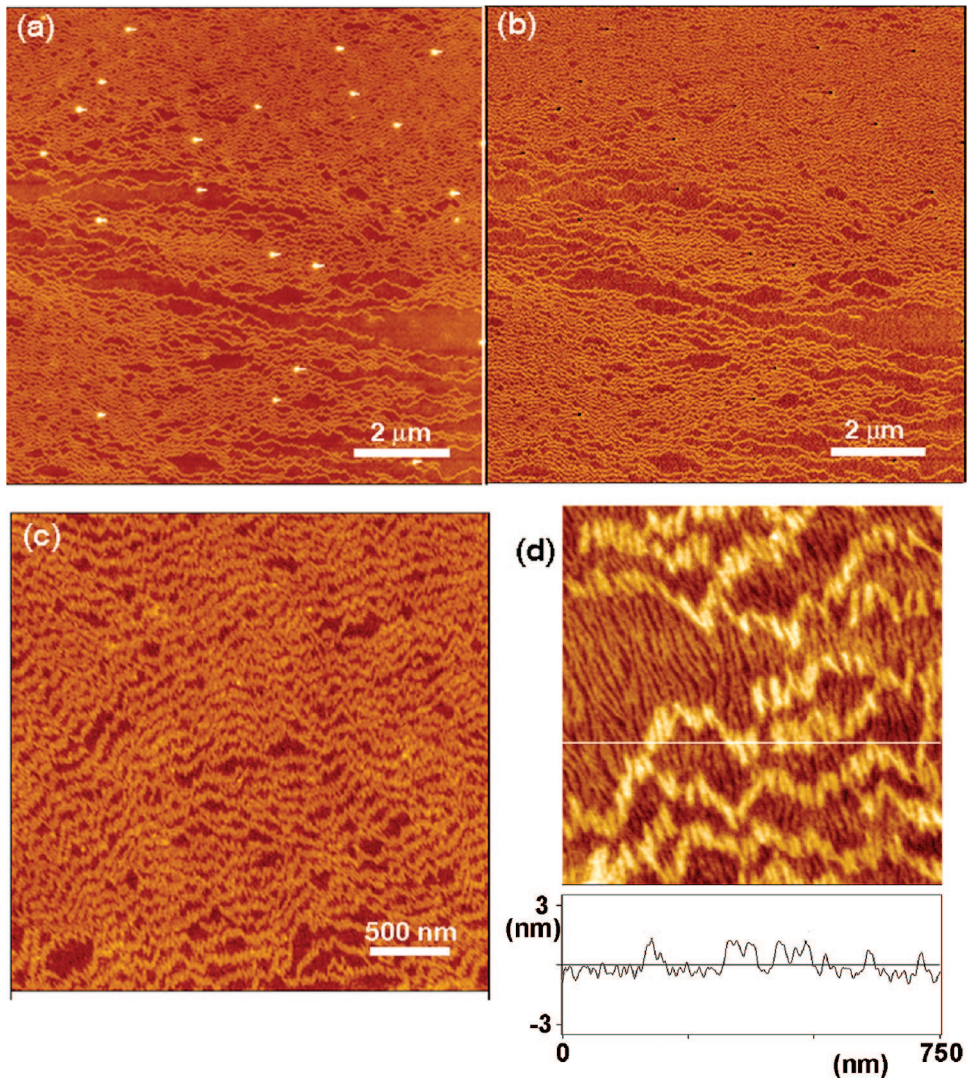

Figure 4. Tapping mode AFM images of smectic-on-nematic bilayer films of the triblock copolymer obtained by annealing for 1 h under THF vapor after dip-coating in 0.5% solutions. (a, b) Low-magnification height and phase contrast images of the bilayered film. (c) A height contrast image of the smectic overlayer. (d) A high-magnification image with a cross-sectional profile of the region showing the nematic bottom layer with smectic overlayer. Note that the entire smectic layer has a uniform thickness of about 1.5 nm, approximately the same as that of the nematic bottom monolayer.

by dip-coating at the copolymer concentration of near 0.1% w/v (Figure 2a) as reported previously.[15] The thickness of the as-coated film was about 1.2−1.5 nm as estimated by the AFM image in Figure 2a. This corresponds approximately to the sum of the chain dimensions of P2VP and PHIC. The thickness of monomolecular P2VP films as adsorbed to mica is known to be 3−4 Å,[30] and the diameter of a PHIC chain in solution is known to be 1.6 nm and becomes about 1 nm when measured for a dry Langmuir–Blodgett film.[32] X-ray photoelectron spectroscopy (XPS) peak of N(1s) resulted in two peaks centered at 399.5 and 401.3 eV, which correspond to the amide group of PHIC and the mica-adsorbed pyridine, respectively.[15]

Increasing the concentration of the copolymers in the dipping solution above 0.1% resulted in the films with a rough surface consisting of the islands of excess copolymer residues, which are not directly adsorbed to the substrate surface, as shown in Figure 2b,c. The film with a greater amount of the island residues (Figure 2c) was obtained by the immersion-coating method to avoid the formation of micelles and precipitates that occurred to the sample dip-coated in high-concentration solutions.

The height contrast AFM image (Figure 2b) of the as-coated film with the islands of copolymer aggregates shows that a layer formed at the bottom similarly to the monolayer of Figure 2a. The islands are the rod−coil block copolymer aggregates physically adsorbed over the bottom monolayer surface. The height of the islands was within 1−3 nm from the bottom layer surface. Because the bottom layer contains holes, which are regions of the bare substrate surface uncovered with the copolymer layer, the thickness of the bottom layer could be estimated to be about 1.0−1.5 nm from its AFM height profile. In Figure 2d is sketched a schematic cross-sectional profile of the monomolecular and bimolecular-thick films (such as Figure 2a,b) in which the upper layer has opposite order of the polymer blocks as compared with the bottom monolayer. The island regions of the film in Figure 2b consist of the surface-adsorbed P2VP, the planar PHIC chains, and the segregated P2VP blocks at the top. The PHIC chains in the intermediate layer may be connected to the top or bottom P2VP blocks. In the case of the film with a greater amount of copolymer top (Figure 2c), the top residues are likely to have incompletely organized structures.

As the as-coated copolymer films exhibiting the images in Figure 2 are exposed to solvent vapor, the solvent molecules adsorb to the film and yield a solvent-swollen, lyotropic liquid crystalline nanofilm on the surface, allowing the copolymer chains to reorganize. Because of the P2VP−mica bonding, the

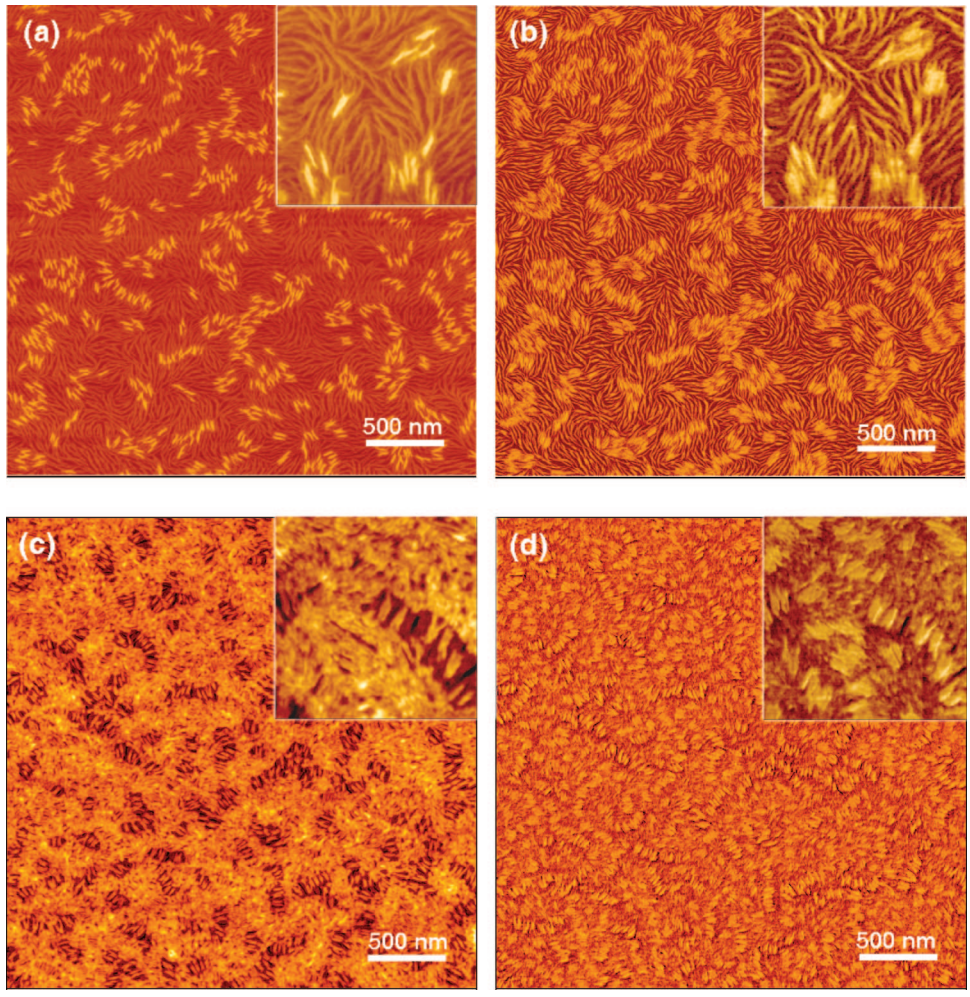

Figure 5. Tapping mode AFM images of the films after annealing in toluene-vapor atmosphere for 1 h: (a, b) the film was dip-coated in 0.1% copolymer toluene solution; (c, d) the film was immersion-coated for 3 h in 0.5% copolymer toluene solution; (a, c) height contrast; (b, d) phase contrast image. Insets are magnified images for an area of 500 × 500 nm^2.

substrate surface is kept wet with the solution layer throughout the annealing procedure. We investigated how the copolymers in the thin films in Figure 2 organized under vapor of three different types of solvents, THF, a good solvent for both of PHIC and P2VP, toluene, a PHIC-selective solvent, and methanol, a P2VP-selective solvent.

In Figure 3 are shown the tapping mode AFM images of the THF vapor-annealed copolymer film with a small amount of excess polymer residue at the top. This morphology was often observed in the films dip-coated in 0.1% copolymer solution which was rinsed incompletely after dip-coating. After annealing the dip-coated film for more than 5 h under THF vapor, the excess copolymer residues reorganized into needle-like nano-objects. The facile reorganization of the copolymer chains over the bottom nematic monolayer is indicative of the formation of a solution layer over the substrate surface under the solvent vapor atmosphere. The formation of the nano-objects is likely a result from crystallization of PHIC chains upon evaporation of solvent from the corresponding lyotropic liquid crystalline layer.

The long axes of the nano-objects were oriented parallel to the director of the bottom nematic layer and arranged side by side in a row running across the director. The nano-objects have thickness of 1−1.5 nm, which is nearly the same as the bottom monolayer thickness, as estimated by the elevation from the bottom PHIC layer in the AFM height profile in Figure 3b. Their length was 60−70 nm, approximately the same as that of an extended PHIC chain with the degree of polymerization (N) of 331 (considering the repeating unit length to be about 0.2 nm, the length of an extended PHIC chain is about 66 nm). The width of the nano-objects was 10−15 nm by the AFM. The lateral size with the presence of tip convolution in mind and the thickness estimated from height image suggest that the nano-object is a monomolecular-thick bundle of several rod−coil block copolymer molecules, as shown in the schematic model in Figure 3c. It is likely that, when several triblock copolymer chains are bundled into a nano-object with thickness of a single chain, they adopt a hairpin-like conformation, as shown in Figure 3d, so that unfavorable extension of P2VP chains, which would occur for z-like conformation, can be avoided. Furthermore, the hairpin-like conformation will help efficient segregation of the P2VP blocks, enabling side by side arrangement of the copolymer chains to bundles and further to a row of bundles. The thickness profile of the whole layer containing the nano-objects was obtained from the film partially scratched off by the contact mode scanning of the AFM (Figure 3e).

In Figure 3f,g are shown the AFM images of the films in the intermediate stage of reorganization, which were sometimes captured from the sample annealed for 1−2 h under the THF vapor. These images show that the PHIC blocks in the bottom layer are already highly oriented before free copolymer chains in the overlayer reorganized completely. The phase contrast image Figure 3f exhibits the segregation of free copolymer chains over the PHIC background is underway.

As the amount of free copolymer chains deposited over the bottom nematic monolayer was increased so as to form many

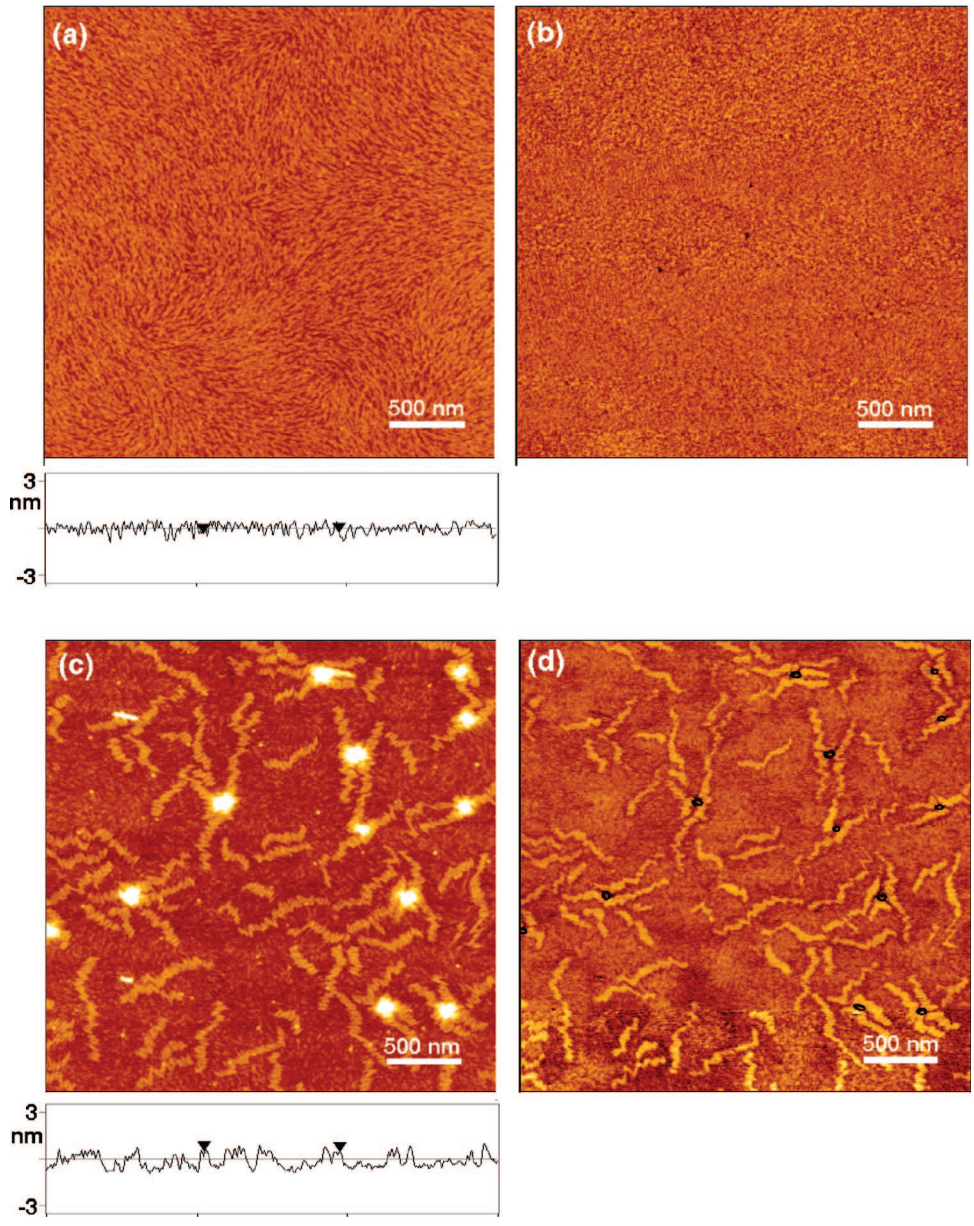

Figure 6. Tapping mode AFM images of densified PHIC nematic bottom layers formed by annealing the as-coated films for 20 h under toluene vapor atmosphere. The films were coated by dip-coating in 0.5% (a, b) and 1% (c, d) copolymer solutions. (a, c) Height contrast; (b, d) phase contrast image.

rod−coil bundles, on annealing with THF vapor, they aligned parallel to each other until they covered almost the entire surface of the nematic bottom layer, as shown in Figure 4. The resulting pattern at the top layer was smectic-like. Low-magnification images in Figure 4a−c exhibit a long-range, unidirectional smectic order in the overlayer, extending over a $10 \times 10\ \mu m^2$ area. The thickness of the smectic layer is about 1.5 nm (Figure 4d), slightly thicker than the isolated nano-objects, likely due to denser packing of the rod−coils in the smectic rows than in isolated bundles. The AFM image in the region not covered with the smectic overlayer shows that the nematic pattern of the bottom layer persisted in the presence of the smectic overlayer. It is noteworthy that the resulting film has a smectic-on-nematic biphasic bilayer structure in a thickness of only about 3 nm. A nanosheet structure of bimolecular packed rods has been predicted by computational study for laterally tethered nanorods.[33]

Long-range smectic arrangement in the overlayer was not observed when the as-coated films were annealed under toluene vapor, which is a rod (PHIC)-selective solvent. The AFM images in Figure 5a,b show that the nanoscale bundles of the copolymer chains are arranged only in a short-range order along the pattern of the bottom nematic monolayer containing a high density of splay and bend deformation. The result is likely an indication that the reorganization of the surface-adsorbed copolymer chains is restricted by the strongly bound P2VP blocks under toluene atmosphere. The copolymer chains that are not directly adsorbed to the substrate surface are free to diffuse and can be rearranged along the curved nematic pattern of the bottom monolayer. This behavior was unchanged by increasing the amount of the copolymer residues in the overlayer as can be seen in Figure 5c,d. Side by side arrangement of the nano-objects occurred locally in the domains under which the bottom layer director were not deformed, resulting in the fragmented smectic stripes distributed over the surface.

An interesting result was obtained when the films were annealed under a toluene atmosphere for a prolonged time. The film which exhibited the morphology in Figure 5 at 1 h

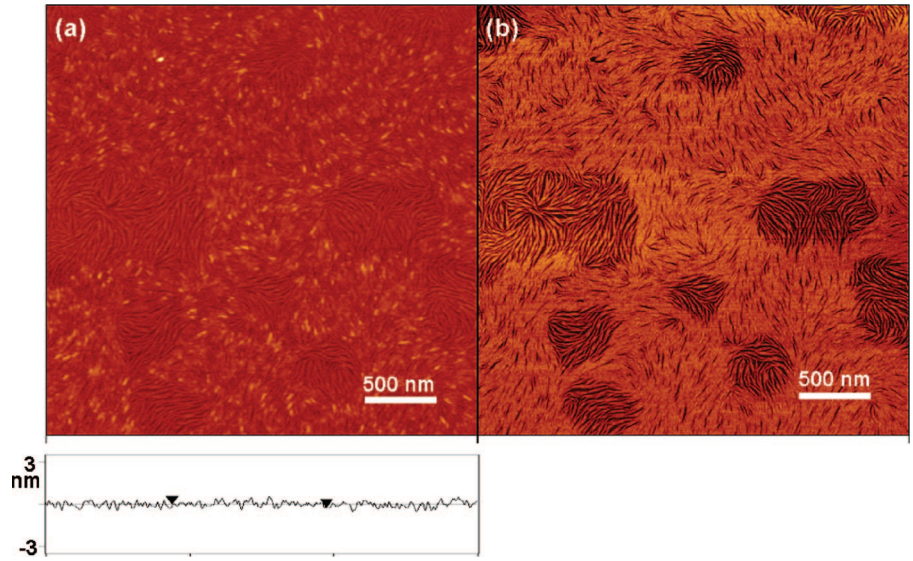

Figure 7. Formation of an inverted nematic monolayer structure observed in the film annealed under methanol vapor which is a selective solvent for coil (P2VP) block: (a) height contrast, (b) phase contrast AFM image for the 0.1% solution dip-coated sample annealed for 20 h under toluene vapor followed by 1 h under methanol vapor.

annealing transformed to a dense layer of PHIC chains after annealing for a sufficiently long time (20 h) under a toluene atmosphere. In Figure 6a,b are shown the AFM images of the monolayer obtained from 20 h toluene vapor annealing of the film dip-coated in a 0.5% w/v copolymer solution. The surface, on which the nanoobjects of the rod−coil bundle are absent, shows a typical nematic texture with very low surface roughness. The corresponding phase contrast image exhibits chemical uniformity of the surface, indicating the film surface consists of only rods (PHIC). This result is attributed to the diffusion of the free rod−coil chains from the overlayer to the bottom layer during toluene vapor annealing and their irreversible adsorption onto the mica surface.

When the amount of free copolymers was increased even further by preparing the film by dip-coating in 1% w/v concentration, all of the free copolymer chains could not diffuse to the substrate surface likely because of saturation of the surface toward adsorption. In addition to the densification of the bottom layer, the excess chains reorganized to islands of short zigzag stripes, distributed randomly over the bottom layer surface, as shown in Figure 6c,d. The random orientation in the bottom layer director and the zigzag stripes indicate that the orientational order in the film plane can be significantly enhanced only when the coil (P2VP) blocks are allowed to desorb from the substrate surface as in the case of THF vapor annealing.

Desorption of the coil (P2VP) blocks from the surface is promoted by annealing the nanofilms under methanol vapor, which is a coil (P2VP)-selective solvent. In Figure 7 is shown the AFM image of the monolayer-thick film after annealing under methanol vapor. Before methanol exposure, the sample was treated under toluene vapor to ensure the formation of the PHIC nematic monolayer that is adsorbed via P2VP−mica bonding. In the films treated with methanol vapor, as shown in the topographic image in Figure 7a, the domains with blurred nematic texture appeared. The phase contrast image in Figure 7b shows clear distinction between different domains, indicating that the blurred topographic region is covered with the P2VP blocks raised over the surface of the PHIC monolayer.

The absence of macroscopic dewetting of the film under methanol vapor is rather surprising considering that the hydrogen bonding between the P2VP and mica can be easily broken by methanol. This may be accounted for by the two-dimensional physical cross-links by the crystalline rod (PHIC) bundles in the nematic monolayer. The pattern with high density of nematic defects indicates that the PHIC layer has not been solublized under a methanol atmosphere.

We investigated the morphology of the films with relatively large amount of copolymer residues by annealing under THF vapor. Annealing the films which was immersion-coated in 0.5% toluene solution (which gives an as-coated morphology similar to Figure 2c) for about 1 h under a THF atmosphere resulted in rough surface morphology with thick and large islands, as shown in Figure 8a. The thickness of some islands of Figure 8a was approximately integer multiple of monomolecular thickness, and some of them exhibited a terraced edge structure (see Supporting Information, Figure S1). A smectic arrangement of the copolymer in the islands is easily visible in the phase contrast image of Figure 8b.

Interestingly, some islands in Figure 8a do not exhibit the smectic stripes in the corresponding phase contrast image in Figure 8b but show curved nematic texture, suggesting that at the early stage of annealing the smectic order is poorly developed in the polymer residues above the deformed nematic bottom layer.

As the films with the islands were annealed further for a prolonged time (20 h) under THF vapor, the film surface became flattened (Figure 8c) in the topography and exhibited a long-range oriented smectic texture in its phase contrast AFM image (Figure 8d). In the phase contrast image, almost the entire surface was covered with the smectic pattern, indicating that the initial nematic residues in the overlayer (as shown in Figure 8a,b) transformed to the smectic state in Figure 8c,d. The planarization may be accounted for by the compatibility between the smectic overlayer and the nematic bottom layer in the long annealed sample, which resulted from the long-range orienational order developed under prolonged exposure to THF vapor.

The images shown above in Figures 2−8 were obtained from the thin films dried after dip- or immersion-coating or solvent vapor treatment. As swollen with the toluene or THF, the PHIC chains may not exist in the form of the crystalline bundles, which made possible to obtain clear height or phase contrast images for the nematic and smectic texture in the thin films. It is most likely that the copolymer chains exist as illustrated in Figure 9, the schematic drawings for the liquid crystalline monolayer and bilayer structures of the amphiphilic rod−coil−rod block copolymer in their solvent-swollen state. It is intriguing that

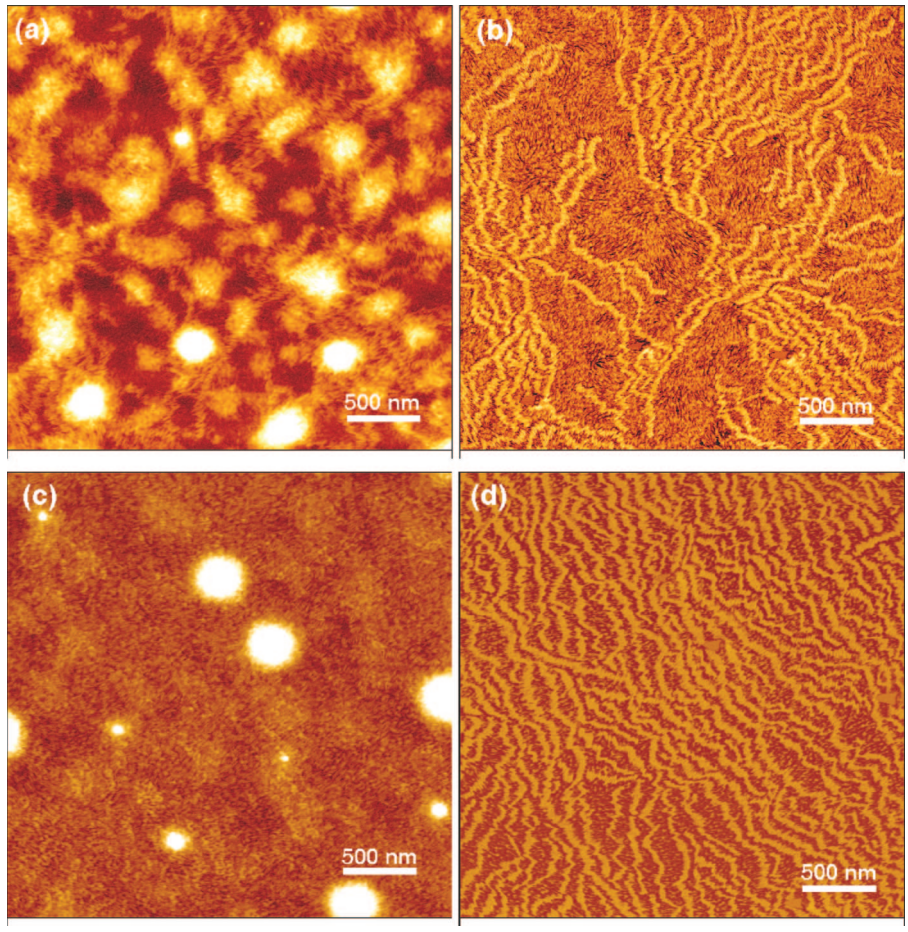

Figure 8. Tapping mode AFM images of the films with smectic layer structures formed on the nematic monolayer surface after annealing the as-coated films with thicker free copolymer residues under THF vapor for different annealing times: (a, b) 1 h and (c, d) 20 h. (a, c) Height contrast images; (b, d) phase contrast images. Corresponding untreated films were obtained by immersion for 3 h in a 0.01% copolymer toluene solution.

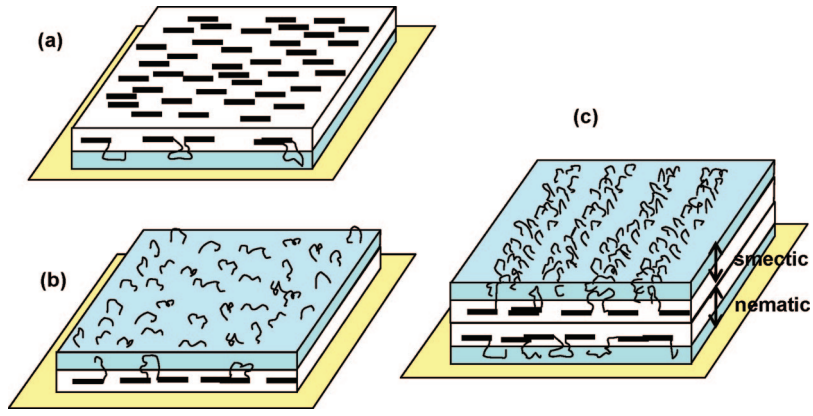

Figure 9. Schematic drawings for the liquid crystalline monolayer and bilayer of the amphiphilic rod−coil−rod block copolymer in their solvent-swollen state on the substrate surface: (a) oriented nematic monolayer under toluene or THF vapor, (b) inverted nematic monolayer under methanol vapor, and (c) oriented smectic-on-nematic bilayer structure under THF vapor.

these structures are analogous to those of self-assembled monolayers or bilayers obtained from small molecule amphiphiles or phospholipids, except for the fact that the hydrophobic part in the present system consists of rodlike polymer chains that organized in liquid crystalline phases.

Conclusion

We obtained several types of liquid crystalline monolayer or bilayer morphologies, including unprecedented smectic-on-nematic biphasic sheet structure, via self-organization of the amphiphilic rod−coil−rod block copolymer in a few nanometers thick films. We have demonstrated that the self-assembly of the rod−coils in a few nanometers thick films can be controlled by adjusting the interaction of each block with the substrate surface and solvents and the amount of deposited copolymers.

The results implicate that other rodlike polymers or inorganic nanoparticles tethered with flexible polymers can show similar self-organizing behaviors on the substrate surface. The unique surface behaviors of amphiphilic rod−coil block copolymers investigated here may be used in designing functional thin films

from many rodlike polymers with electronic or biological properties.

Acknowledgment. This work was supported by the Korea Research Foundation Grant Funded by the Korean Government (KRF-2005-205-D00035) and the Program for Integrated Molecular Systems at Gwangju Institute of Science and Technology in Korea.

Supporting Information Available: AFM image of the film with the smectic islands exhibiting terraced edge. This material is available free of charge via the Internet at http://pubs.acs.org.

References and Notes

(1) Chen, J. T.; Thomas, E. L.; Ober, C. K.; Mao, G.-p. *Science* **1996**, *273*, 343.
(2) Chen, X. L.; Jenekhe, S. A. *Macromolecules* **2000**, *33*, 4610.
(3) Cornelissen, J. J. L. M.; Fischer, M.; Sommerdijk, N. A. J. M.; Nolte, R. J. M. *Science* **1998**, *280*, 1427.
(4) Lee, M.; Cho, B.-K.; Zin, W.-C. *Chem. Rev.* **2001**, *101*, 3869.
(5) Tenneti, K. K.; Chen, X. F.; Li, C. Y.; Tu, Y. F.; Wan, X. H.; Zhou, Q. F.; Sics, I.; Hsiao, B. S. *J. Am. Chem. Soc.* **2005**, *127*, 15481.
(6) Jenekhe, S. A.; Chen, X. L. *Science* **1998**, *279*, 1903.
(7) Agut, W.; Taton, D.; Lecommandoux, S. *Macromolecules* **2007**, *40*, 5653.
(8) Sary, N.; Mezzenga, R.; Brochon, C.; Hadziioannou, G.; Ruokolainen, J. *Macromolecules* **2007**, *40*, 3277.
(9) Park, J. W.; Thomas, E. L. *Macromolecules* **2006**, *39*, 4650.
(10) Sary, N.; Rubatat, L.; Brochon, C.; Hadziioannou, G.; Ruokolainen, J.; Mezzenga, R. *Macromolecules* **2007**, *40*, 6990.
(11) Wang, H. B.; Jost, R.; Wudl, F. *J. Polym. Sci., Polym. Chem.* **2007**, *45*, 800.
(12) Tao, Y. F.; Zohar, H.; Olsen, B. D.; Segalman, R. A. *Nano Lett.* **2007**, *7*, 2742.
(13) Olsen, B. D.; Segalman, R. A. *Macromolecules* **2007**, *40*, 6922.
(14) Park, J. W.; Cho, Y. H. *Langmuir* **2006**, *22*, 10898.
(15) Kim, J. H.; Rahman, M. S.; Lee, J. S.; Park, J. W. *J. Am. Chem. Soc.* **2007**, *129*, 7756.
(16) Vriezema, D. M.; Hoogboom, J.; Velonia, K.; Takazawa, K.; Christianen, P. C. M.; Maan, J. C.; Rowan, A. E.; Nolte, R. J. M. *Angew. Chem., Int. Ed.* **2003**, *42*, 772.
(17) Matsen, M. W.; Barrett, C. *J. Chem. Phys.* **1998**, *109*, 4108.
(18) Halperin, A. *Europhys. Lett.* **1989**, *10*, 549.
(19) Halperin, A. *Macromolecules* **1990**, *23*, 2724.
(20) Schleuss, T. W.; Abbel, R.; Gross, M.; Schollmeyer, D.; Frey, H.; Maskos, M.; Berger, R.; Kilbinger, A. F. M. *Angew. Chem., Int. Ed.* **2006**, *45*, 2969.
(21) Mao, M.; Turner, S. R. *J. Am. Chem. Soc.* **2007**, *129*, 3832.
(22) Park, J. W.; Thomas, E. L. *Adv. Mater.* **2003**, *15*, 585.
(23) Olsen, B. D.; Li, X. F.; Wang, J.; Segalman, R. A. *Macromolecules* **2007**, *40*, 3287.
(24) Russell, T. P. *Curr. Opin. Colloid Interface Sci.* **1996**, *1*, 107.
(25) Hawker, C. J.; Russell, T. P. *MRS Bull.* **2005**, *30*, 952.
(26) Muthukumar, M.; Ober, C. K.; Thomas, E. L. *Science* **1997**, *277*, 1225.
(27) Park, J.-W.; Thomas, E. L. *J. Am. Chem. Soc.* **2002**, *124*, 514.
(28) Shin, Y. D.; Han, S. H.; Samal, S.; Lee, J. S. *J. Polym. Sci., Polym. Chem.* **2005**, *43*, 607.
(29) Rahman, M. S.; Samal, S.; Lee, J. S. *Macromolecules* **2006**, *39*, 5009.
(30) Spatz, J. P.; Moller, M.; Noeske, M.; Behm, R. J.; Pietralla, M. *Macromolecules* **1997**, *30*, 3874.
(31) Green, M. M.; Peterson, N. C.; Sato, T.; Teramoto, A.; Cook, R.; Lifson, S. *Science* **1995**, *268*, 1860.
(32) Ohkita, M.; Higuchi, M.; Kawaguchi, M. *J. Colloid Interface Sci.* **2005**, *292*, 300.
(33) Horsch, M. A.; Zhang, Z.; Glotzer, S. C. *Nano Lett.* **2006**, *6*, 2406.

MA702695A